Popul Ecol (2014) 56:401–415
DOI 10.1007/s10144-013-0428-8

THE SOCIETY OF POPULATION ECOLOGY

ORIGINAL ARTICLE

A moving–resting process with an embedded Brownian motion for animal movements

Jun Yan · Yung-wei Chen · Kirstin Lawrence-Apfel · Isaac M. Ortega · Vladimir Pozdnyakov · Scott Williams · Thomas Meyer

Received: 29 June 2013 / Accepted: 11 December 2013 / Published online: 29 January 2014

Abstract Animal movements are of great importance in studying home ranges, migration routes, resource selection, and social interactions. The Global Positioning System provides relatively continuous animal tracking over time and long distances. Nevertheless, the continuous trajectory of an animal's movement is usually only observed at discrete time points. Brownian bridge models have been used to model movement of an animal between two observed locations within a reasonably short time interval. Assuming that animals are in perpetual motion, these models ignore inactivity such as resting or sleeping. Using the latest developments in applied probability, we propose a moving–resting process model where an animal is assumed to alternate between a moving state, during which it moves in a Brownian motion, and a resting state, during which it does not move. Theoretical properties of the process are studied as a first step towards more realistic models for animal movements. Analytic expressions are derived for the distribution of one increment and two consecutive increments, and are validated with simulations. The induced bridge model conditioning on the starting and end points is used to compute an animal's probability of occurrence in an observation area during the time of observation, which has wide applications in wildlife behavior research.

Keywords Alternating renewal process · Brownian bridge · Home range · Poisson process · Stationary

J. Yan (✉) · Y. Chen · V. Pozdnyakov
Department of Statistics, University of Connecticut, Storrs, USA
e-mail: jun.yan@uconn.edu

J. Yan · I. M. Ortega · T. Meyer
Center for Environmental Sciences and Engineering, University of Connecticut, Storrs, USA

K. Lawrence-Apfel · I. M. Ortega · T. Meyer
Department of Natural Resources and the Environment, University of Connecticut, Storrs, USA

S. Williams
Department of Forestry and Horticulture, Connecticut Agricultural Experiment Station, New Haven, USA

Introduction

Wildlife biologists have long depended on remote monitoring of individual animals to determine movements, behaviors, and home ranges (Heezen and Tester 1967; Marshall and Whittington 1969; Hutton et al. 1976; Dunn and Gipson 1977). Animals move in continuous trajectories through their environment. Although new technologies allow for global positioning system (GPS) devices that sample near-continuous tracks of animal positions, devices with solar charging batteries are dependent on the weather; and studies using devices with non-solar batteries for near-continuous tracks are short in duration (generally less than one month) because of rapid battery depletion. If year-round, seasonal movement data are required, this can become invasive and prohibitively expensive due to the need to recapture animals and refurbish batteries on animal-carried devices. The continuous track, if available, can be used to validate any animal movement model that use discretely observed data as input. More generally in practice, the continuous trajectory of animal movements is only observed at a collection of discrete times. This leads to a problem of interpolation, or estimation, of an animal's path between two consecutive observations, which provide limits on an animal's location during the intervening time when no positions are known.

The Brownian bridge movement model (BBMM) is an approach that models the missing movement path between two sequential positions by a Brownian bridge (Horne et al. 2007). A Brownian bridge is a stochastic process derived from a Brownian motion; its distribution is the conditional distribution of a Brownian motion given the locations at a beginning time and an ending time. It is a conditional random walk between successive pairs of locations, dependent on the time between locations, the distance between locations, and the Brownian motion variance which characterizes the animal's mobility. Although the BBMM can be appropriate for migratory behavior (White et al. 2010), it assumes a single animal movement pattern—the motion is characterized by only a single mobility parameter. This is unrealistic, especially when the animal journey is long. An animal can have different levels of mobility and activity–inactivity periods influenced by food availability, predation risk, season, time-of-day, social behavior, and reproductive periods; some activities cause animals to be diurnal, nocturnal, or crepuscular (Zschille et al. 2010). To accommodate behaviorally distinct mobility levels, Benhamou (2011) expanded the BBMM with different but constant variance parameters, which characterize mobility, for advection and diffusion and for different habitats. Kranstauber et al. (2012) proposed a dynamic extension of the BBMM where the variance parameter is allowed to change dynamically along a path, and the change points are estimated with likelihood comparisons in a moving window (Gurarie et al. 2009).

One aspect that has not been studied is inactivity period, which would correspond to zero variance in a BBMM. Animals use inactivity periods for sleeping, ruminating, vigilance, hibernating, or resting without sleeping. Sleep time in mammals varies from fewer than 3 h to more than 20 h per day (Siegel 2009). Although some vertebrates were reported to be in continuous motion (Kavanau 1998), some mammals spend as much as 75 % of their time inactive (Wilson et al. 2009; Giné et al. 2012). At fine temporal scales, a realistic stochastic model should include inactivity periods. The dynamic BBMM of Kranstauber et al. (2012) may accommodate inactivity periods to some extent by a variance parameter approaching zero (nonetheless not equal to zero), but conceptually, it still assumes perpetual movement, just in different mobility.

With recent advances in applied probability, we propose an alternative model that allows an animal to stop moving at a random time and stay still for a random length of period. Important properties of the process are studied as the first step towards a more realistic and theoretically sound model for animal movements for practical usage. Our model has an underlying alternating renewal process that governs two phases: moving and resting. Some animals, like most sharks, move while they rest but we use "resting" simply to mean periods when an animal is not moving. The alternating renewal process, also known as the telegraph process or the on–off process, was first studied by Cane (1959) and Page (1960) in the context of animal ethology and maintenance of electronic equipment, respectively. Mathematically this is not a trivial object, and as a result, this area of research is still quite active. In particular, in our analysis we used results from work of Perry et al. (1999), Stadje and Zacks (2004), Zacks (2004), and Di Crescenzo et al. (2005). For our model, the durations of moving and resting periods are random. Obtaining a solvable analytical model requires modeling the time periods with exponential distributions (Zacks 2004). The average time spent in moving and resting phases can be different. During the resting phase, animal location does not change. During the moving phase, the Brownian motion model is used, and to build up the foundations for further generalizations, we assume a single movement pattern with a single variance parameter. The model is implemented in an R package `smam` (Yan and Pozdnyakov 2013) for statistical modeling of animal movement.

This article is organized as follows. The moving–resting process and the alternating renewal process are presented in the next section along with their intuitive properties. The bridge model resulting from a moving–resting process is then derived based on the marginal distributions of one-time increment and bivariate two-consecutive-time increments of the process. The next section provides an example of application of the model in animal movements to occupation time distribution with two observed ending points of a time interval. Parameter estimation is then presented with two cases depending on whether or not the moving–resting state is observed. The model is illustrated with data from a female mountain lion (*Puma concolor*). A discussion on limitations and extensions concludes the last section.

Moving–resting process

Our moving–resting model modifies the BBMM by adding periods of inactivity. The active periods and inactive periods are modeled by an alternating renewal process with exponentially distributed holding times. Let $\{M_i\}_{i \geq 1}$ be independent and identically distributed (i.i.d.) random variables with exponential distribution with mean $1/\lambda_m$ and $\{R_i\}_{i \geq 1}$ be i.i.d. random variables with exponential distribution with mean $1/\lambda_r$. Assume that $\{M_i\}_{i \geq 1}$ and $\{R_i\}_{i \geq 1}$ are independent. Consider an alternating renewal process that with probability p_m, $0 \leq p_m \leq 1$ starts with a *moving* cycle (i.e., we have $M_1, R_1, M_2, R_2, \ldots$) and with probability $p_r = 1 - p_m$ starts with *resting* cycle (i.e., we

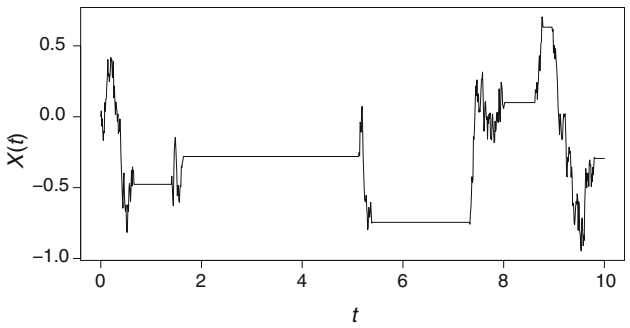

Fig. 1 A realization from a one-dimensional ($d = 1$) moving–resting process with $(\sigma, \lambda_m, \lambda_r) = (1, 1, 1)$ over $t \in (0, 10)$. The straight line segments represent the time period in which the process is inactive

have $R_1, M_1, R_2, M_2, \ldots$). With the exponentially distributed renewal times, the marginal probability that the process is in the moving phase and that the process is in the resting phase are, respectively,

$$p_m = \frac{\lambda_r}{\lambda_m + \lambda_r} \quad \text{and} \quad p_r = \frac{\lambda_m}{\lambda_m + \lambda_r}.$$

Let $S(t)$, $t \geq 0$ be the state process; that is, $S(t) = 1$ if the alternating renewal process is in a moving cycle and $S(t) = 0$ if the process is in a resting cycle at time t. Let $X(t)$ be a d-dimensional moving–resting process indexed by time $t > 0$. Conditioning on the state of the underlying renewal process, $S(t)$, the moving–resting process $X(t)$ is defined by the stochastic differential equation

$$\mathrm{d}X(t) = \begin{cases} \sigma \mathrm{d}B(t) & S(t) = 1, \\ 0 & S(t) = 0, \end{cases} \tag{1}$$

where σ is a volatility parameter, and $B(t)$ is the standard Brownian motion. The process is characterized by three parameters $(\sigma, \lambda_m, \lambda_r)$.

Simulation from the moving–resting process model after it is already stationary is straightforward with the following algorithm:

1. With probability p_m and p_r, respectively, start from moving and resting phase at $t = 0$.
2. Generate the alternating renewal process with exponential distributions with rate λ_m and λ_r.
3. Remove the resting periods and fill the moving periods with a Brownian motion with volatility σ.
4. Fill each resting period with its initial location.

Figure 1 shows a realization from a moving–resting process in the one-dimensional case ($d = 1$) with $(\sigma, \lambda_m, \lambda_r) = (1, 1, 1)$ starting from a moving state ($S(0) = 1$). If we let this process evolve for a very long time, the probability that it is in the moving phase and that in the resting phase at a random time point will be $p_m = 1/2$ and $p_r = 1/2$, respectively.

Let $M(t)$ and $R(t)$, $t > 0$ be the total time in interval $(0, t]$ spent in the moving cycles and in the resting cycles, respectively; consequently, $R(t) = t - M(t)$. For a given initial state $S(0)$, the most important quantity in analyzing the alternating process is the joint distributions of the two pairs $(M(t), S(t))$ and $(R(t), S(t))$. First, it is known that in the case when durations of alternating phases are described by exponential distributions, closed-form expressions for their densities are available (e.g., Zacks 2004, p. 500). The second important observation is the Markov property of the location/phase state process; that is, because of the memoryless property of the exponential distribution and the Markov property of the Brownian motion, the joint process $\{X(t), S(t): t \geq 0\}$ is a Markov process with stationary increments in $X(t)$. Combining these two facts together, an explicit formula for the joint density $\Pr[X(s) \in \mathrm{d}x, X(t) - X(s) \in \mathrm{d}y], 0 < s < t$, can be derived as long as we have the joint "densities" for $X(t)$ and $S(t)$; see Section "Bridge model from moving–resting process" for details.

Mathematically, Brownian motion is a special case of the moving–resting process when there is no resting phase—$\lambda_r \to \infty$. Our model has some features that are impossible to accommodate within the framework of the Brownian motion. One is, of course, staying in one location during a resting phase. There are other, less apparent, but interesting characteristics. For example, consider the 2-dimensional case with coordinates (x, y). For a moving–resting process, the observed x- and y-coordinates are not independent, as opposed to the independence in a Brownian motion. The x-movements and y-movements are inherently synchronized so that they have the same state process at all time points. Consequently, the shared resting phases introduces dependence between x- and y-locations. Indeed, if we have an exactly zero x-movements, then it means that an animal rested during this time period, and, as a result, the corresponding y-movements will be zero too.

In spite of the added complexity, the model is tractable. Recent theoretical findings on alternating renewal processes (Perry et al. 1999; Stadje and Zacks 2004; Zacks 2004; Di Crescenzo et al. 2005)—more specifically, $M(t)$ and $R(t)$—facilitate closed-form formulas for the moving–resting process; see next section for more details. Define

$$P_m[\cdot] = \Pr[\cdot | S(0) = 1], \quad \text{and} \quad P_r[\cdot] = \Pr[\cdot | S(0) = 0].$$

Then, for $0 < w < t$, we introduce the following (defective) densities

$$\begin{aligned} p_{mm}(w, t)\mathrm{d}w &= P_m[M(t) \in \mathrm{d}w, S(t) = 1], \\ p_{mr}(w, t)\mathrm{d}w &= P_m[M(t) \in \mathrm{d}w, S(t) = 0], \\ p_{rm}(w, t)\mathrm{d}w &= P_r[R(t) \in \mathrm{d}w, S(t) = 1], \\ p_{rr}(w, t)\mathrm{d}w &= P_r[R(t) \in \mathrm{d}w, S(t) = 0]. \end{aligned}$$

According to Zacks (2004, p.500), we have that

$$p_{mm}(w,t)=e^{-\lambda_m w-\lambda_r(t-w)}\sum_{n=1}^{\infty}\frac{\lambda_m^n\lambda_r^n}{n!(n-1)!}w^n(t-w)^{n-1},$$

$$p_{mr}(w,t)=\lambda_m e^{-\lambda_m w-\lambda_r(t-w)}+\lambda_m\sum_{n=1}^{\infty}p(n,\lambda_m w)p(n,\lambda_r(t-w)),$$

where $p(n,\ \mu) = e^{-\mu}\mu^n/n!$ is the probability mass function of a Poisson variable with mean μ evaluated at n. Respectively, we have that

$$p_{rr}(w,t)=e^{-\lambda_r w-\lambda_m(t-w)}\sum_{n=1}^{\infty}\frac{\lambda_r^n\lambda_m^n}{n!(n-1)!}w^n(t-w)^{n-1},$$

$$p_{rm}(w,t)=\lambda_r e^{-\lambda_r w-\lambda_m(t-w)}+\lambda_r\sum_{n=1}^{\infty}p(n,\lambda_r w)p(n,\lambda_m(t-w)).$$

It is easy to see that $M(t)$ and $R(t)$ have atoms or point masses at $w = t$ in the following sense:

$$P_m[M(t)=t]=e^{-\lambda_m t}\quad\text{and}\quad P_r[R(t)=t]=e^{-\lambda_r t}.$$

These formulas avoid the demanding task of computing the distribution of the time spent in the moving or resting phase via large scale simulations. The series in the formulas can be evaluated conveniently using the modified Bessel function of the first kind

$$I(z;\alpha)=\sum_{m=0}^{\infty}\frac{\left(\frac{z}{2}\right)^{2m+\alpha}}{m!\Gamma(m+\alpha+1)}.$$

For example, we have $p_{mm}(w,t) = e^{-\lambda_r w-\lambda_m(t-w)}\sqrt{\lambda_m\lambda_r w/(t-w)}I(z;1)$ and $p_{mr}(w,t) = \lambda_m e^{-\lambda_r w-\lambda_m(t-w)}I(z;0)$, where $z = 2\sqrt{\lambda_m\lambda_r w(t-w)}$. Similar forms can be found for p_{rr} and p_{rm}.

Bridge model from moving–resting process

Time spent in moving or resting phase

The time an animal spent in moving and/or resting phases determines the utilization distribution for a given period of time. This feature is completely controlled by the alternating renewal process with parameters (λ_m, λ_r). Assuming that the process $X(t)$ started from $t = -\infty$ and that it has already reached stationarity by time $t = 0$. Therefore, the marginal probabilities of $S(0) = 1$ and $S(0) = 0$ are, respectively, p_m and p_r. Given a time interval $(0, t)$, the time an animal spent in the moving phase during the interval has a (defective) density

$$\begin{aligned}\Pr[M(t)\in \mathrm{d}w] &= p_m[p_{mm}(w,t)\mathrm{d}w+p_{mr}(w,t)\mathrm{d}w]\\ &+p_r[p_{rr}(t-w,t)\mathrm{d}(t-w)+p_{rm}(t-w,t)\mathrm{d}(t-w)]\end{aligned}$$

for $w \in (0, t)$ and an atom at $w = t$. Note that this probability is the same as $\Pr[R(t) \in \mathrm{d}(t - w)]$. For the BBMM, $\Pr[M(t) = t] = 1$ and $\Pr[R(t) = 0] = 1$. These probability characteristics describe the difference between the moving–resting process and the BBMM. In applications to home range analysis, they lead to a tighter possible range than what is implied by a BBMM with the same volatility parameter σ.

Figure 2 shows the density of the time spent moving by time t, $M(t)$, with $t = 10$, $\lambda_m = 1$ and $\lambda_r \in \{1/2, 1, 2\}$. Note that the densities do not integrate to one because of the atom at t and 0, respectively, when $S(0) = 1$ and $S(0) = 0$. When the starting state is moving ($S(0) = 1$), the weight of the atom point t is $\exp(-\lambda_m t)$ regardless of λ_r. On the other hand, when the starting state is resting ($S(0) = 0$), the weight of the atom point 0 is $\exp(-\lambda_r t)$; the smaller λ_r, the longer the resting periods on average, and hence the more weight at 0 for the time in moving. In the extreme case $\lambda_r \to \infty$, the moving–resting process would become Brownian motion, in which case, $M(t)$ is singular at t with weight one for both $S(0) = 1$ and $S(0) = 0$. It is also interesting to note that the density with the same λ_r has more concentration on lower duration values for $S(0) = 0$ than with $S(1) = 1$, because starting from resting would lead to less time for moving on average.

Marginal distribution of one increment

Without loss of generality, we assume $X(0) = 0$. Our first goal is to find the marginal distribution of $X(t)$, $t > 0$. This is the distribution of the animal's location at time t relative to the starting location at time 0, or increment since time 0. The density of this distribution can be derived if we have the joint distribution of $X(t)$ and $S(t)$, $t > 0$. Note that, if the resting phases were removed, then the remaining process is exactly a Brownian motion. For example, for $0 < w < t$,

$$\begin{aligned}P_m[X(t)\in \mathrm{d}x, S(t)=1, M(t)\in \mathrm{d}w]\\ =\phi(x;\sigma^2 w)p_{mm}(w,t)\mathrm{d}x\mathrm{d}w,\end{aligned}$$

where $\phi(\cdot; a)$ is the density function of a normal variable with mean zero and variance a. Note that the normal density ϕ can be univariate, bivariate, or of higher dimension, the same as the dimension of the Brownian motion; the formulas in the sequel remain unchanged. The joint distribution of $(X(t), S(t))$ starting from $S(0) = 1$ can be obtained by integrating w out. Other scenarios can be similarly handled. For ease of notation, let

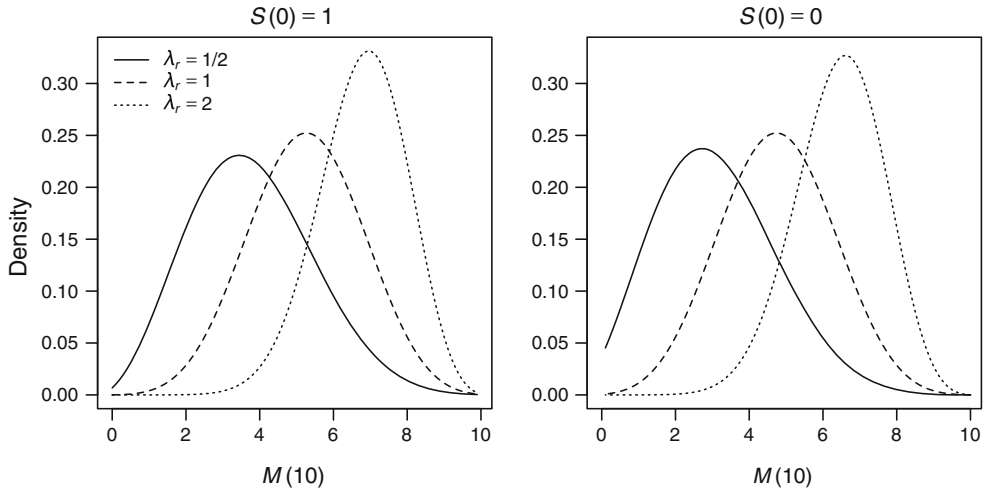

Fig. 2 Density of $M(10)$, the time spent moving for a moving–resting process with $\lambda_m = 1$ and $\lambda_r \in \{1/2, 1, 2\}$ during time interval (0, 10). *Left* starting from moving ($S(0) = 1$). *Right* starting from resting ($S(0) = 0$)

$$h_{mm}(x,t) = e^{-\lambda_m t}\phi(x;\sigma^2 t) + \int_0^t \phi(x;\sigma^2 w)p_{mm}(w,t)\mathrm{d}w,$$

$$h_{mr}(x,t) = \int_0^t \phi(x;\sigma^2 w)p_{mr}(w,t)\mathrm{d}w,$$

$$h_{rr}(x,t) = \int_0^t \phi\big(x;\sigma^2(t-w)\big)p_{rr}(w,t)\mathrm{d}w,$$

$$h_{rm}(x,t) = \int_0^t \phi\big(x;\sigma^2(t-w)\big)p_{rm}(w,t)\mathrm{d}w.$$

Then we have

$$P_m[X(t) \in \mathrm{d}x, S(t) = 1] = h_{mm}(x,t)\mathrm{d}x,$$
$$P_m[X(t) \in \mathrm{d}x, S(t) = 0] = h_{mr}(x,t)\mathrm{d}x,$$
$$P_r[X(t) \in \mathrm{d}x, S(t) = 0] = h_{rr}(x,t)\mathrm{d}x + e^{-\lambda_r t}\delta_0(x),$$
$$P_r[X(t) \in \mathrm{d}x, S(t) = 1] = h_{rm}(x,t)\mathrm{d}x,$$

where $\delta_0(x)$ is the delta function with an atom at 0. Note that the extra part in $P_r[X(t) \in \mathrm{d}x, S(t) = 0]$, $e^{-\lambda_r t}\delta_0(x)$, is the probability that the whole time period $(0, t]$ is in a resting phase. The extra part in $h_{mm}(x,t)$, $e^{-\lambda_m t}\phi(x;\sigma^2 t)$, comes from the possibility that the whole $(0,t]$ interval belongs to a single moving phase.

The marginal density of $X(t)$ is, for any $x \neq 0$,

$$\Pr[X(t) \in \mathrm{d}x]/\mathrm{d}x = p_m h_m(x,t) + p_r h_r(x,t), \quad (2)$$

where $h_m(x, t) = h_{mm}(x, t) + h_{mr}(x, t)$, and $h_r(x, t) = h_{rm}(x, t) + h_{rr}(x, t)$.

The marginal distribution has a point mass at $x = 0$ with probability

$$\Pr[X(t) = 0] = p_r e^{-\lambda_r t}\delta_0(x).$$

This can only happen when the animal starts from the resting phase and stays in it during the whole period $(0,t]$. It is easy to verify that $\int_{-\infty}^{\infty} h_m(x,t)\mathrm{d}x = 1$ and $\int_{-\infty}^{\infty} h_r(x,t)\mathrm{d}x + e^{-\lambda_r t} = 1$.

The marginal distribution of $X(t)$ of the moving–resting process is expected to have a thinner tail than that of Brownian motion, and to have an atom at zero. These facts lead to tighter home range in applications. The probability of the atom at zero depends on the rate of the exponential distributed duration in the resting phase. The smaller the rate, the bigger the probability.

For illustration, we plot the marginal density of $X(t)$ for $t = 10$ with $\sigma = 1$, $\lambda_m = 1$, $\lambda_r \in \{1/2, 1, 2\}$, and $S(0) \in \{1, 0\}$ in Fig. 3. As a reference, we also plotted the density of $X(10)$ for the Brownian motion with $\sigma = 1$, which corresponds to the moving–resting process with $\lambda_r = \infty$. Clearly, the marginal densities of the moving–resting process have thinner tails than that of the Brownian motion. The smaller λ_r, the thinner the tails. The densities with the same λ_r have more concentration around zero for $S(0) = 0$ than those for $S(0) = 1$, which is expected because starting with resting means less movement. For $S(0) = 0$, the densities have an atom at zero with weight $\exp(-\lambda_r t)$, which would show more obviously for smaller t. Further, note that the densities for $S(0) = 0$ might not be differentiable at zero—the peak is obvious for $\lambda_r = 1/2$. As a result, the density of $X(t)$ after $S(0)$ is marginalized out might not be differentiable at zero either.

Joint distribution of two consecutive increments

For $0 < u < t$ and $-\infty < x, y < \infty$, consider the joint distribution of the increment at time u and at time t, $\{X(u), X(t) - X(u)\}$. We have

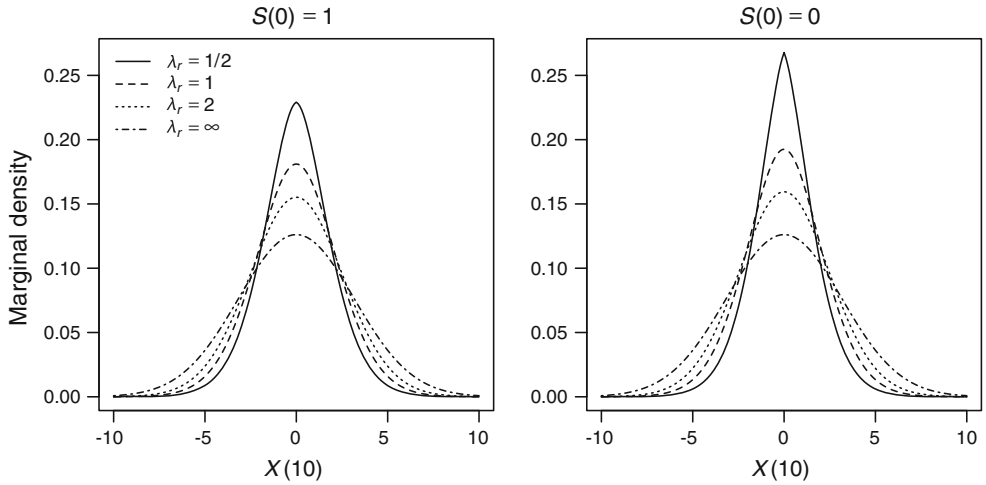

Fig. 3 Marginal density of $X(10)$ for a one dimensional moving–resting process with $\sigma = 1$, $\lambda_m = 1$, and $\lambda_r \in \{1/2, 1, 2\}$. *Left* starting from moving ($S(0) = 1$). *Right* starting from resting ($S(0) = 0$)

$$\begin{aligned}&\Pr[X(u) \in \mathrm{d}x, X(t) - X(u) \in \mathrm{d}y]\\ &= p_m P_m[X(u) \in \mathrm{d}x, X(t) - X(u) \in \mathrm{d}y]\\ &\quad + p_r P_r[X(u) \in \mathrm{d}x, X(t) - X(u) \in \mathrm{d}y].\end{aligned}$$

Because of the memoryless property of the exponential distribution and Markov property of the Brownian motion, the joint process $\{X(t),\ S(t)\}_{t \geq 0}$ is a Markov process. Therefore, for any $x \neq 0$ and $y \neq 0$, we have

$$\begin{aligned}&P_m[X(u) \in \mathrm{d}x, X(t) - X(u) \in \mathrm{d}y]\\ &= P_m[X(t-u) \in \mathrm{d}y] P_m[X(u) \in \mathrm{d}x, S(u) = 1]\\ &\quad + P_r[X(t-u) \in \mathrm{d}y] P_m[X(u) \in \mathrm{d}x, S(u) = 0].\end{aligned}$$

In the same fashion, we get that

$$\begin{aligned}&P_r[X(u) \in \mathrm{d}x, X(t) - X(u) \in \mathrm{d}y]\\ &= P_m[X(t-u) \in \mathrm{d}y] P_r[X(u) \in \mathrm{d}x, S(u) = 1]\\ &\quad + P_r[X(t-u) \in \mathrm{d}y] P_r[X(u) \in \mathrm{d}x, S(u) = 0].\end{aligned}$$

All the terms involved are already available from the last subsection.

Note that this joint distribution has singularity at point $(x, y) = (0, 0)$ and on lines $x = 0$ and $y = 0$. The formulas above are still valid with our notation. Point (0, 0) means that the process started from resting and stayed in the resting phase during the whole time interval $(0, t)$. Line $x = 0$ means that the process started from resting, stayed in resting until at least time u, and moved during (u, t). Line $y = 0$ means that the process moved during $(0, u)$, was in the resting phase at time u, and stayed in the resting phase during (u, t).

Continuing with our illustration, consider the joint distribution of $X(u)$ and $X(t) - X(u)$ with $u = 5$ and $t = 10$ in the one-dimensional case with $\sigma = 1$, $\lambda_m = 1$, $\lambda_r \in \{1/2, 1, 2\}$, and $S(0) \in \{1, 0\}$. We plot the contours of the nonsingular part of the joint density under all scenarios in Fig. 4. To validate the correctness of the formulas, we simulated 10,000 replicates of the process for each scenario, and estimated the nonsingular part of the joint density of $(X(u), X(t) - X(u))$ by bivariate kernel smoothing. The contours of the estimated kernel densities matched those from our formulas closely (the overlaid plots not shown). It is of interest to note that, at $x = 0$ and $y = 0$, the contours appear to have angles instead of being smooth. This is a result of the resting period, similar to the nonsmooth curvature for $S(0) = 0$ in Fig. 3.

The time durations of the two increments are both 5. When $S(0) = 1$ (starting from moving), the range of $X(5)$ (horizontal) is wider than the range of $X(10) - X(5)$ (vertical) for all three λ_r values because, at $t = 5$, the process might be in a resting phase—$S(5) = 0$. When $S(0) = 0$ (starting from resting), the opposite is true. The difference decreases as λ_r increases; when $\lambda_r \to \infty$, the process reduces to a Brownian motion and the two increments have identical distributions.

Bridge distribution

The probability distribution conditioned on starting and ending points is important in applications such as home range analysis (Horne et al. 2007) and analysis of animal movements (e.g., Sawyer et al. 2009). Given $X(0) = 0$ and $X(t) = x$, we seek the conditional distribution of $X(u)$ for $0 < u < t$ that characterizes the bridge model with fixed starting and ending points for the moving–resting process.

It is clear that $P(X(u) = x \mid X(t) = 0) = \delta_0(x)$, because event $X(t) = 0$ can only occur with a positive probability if the whole time period $(0, t]$ is a resting period.

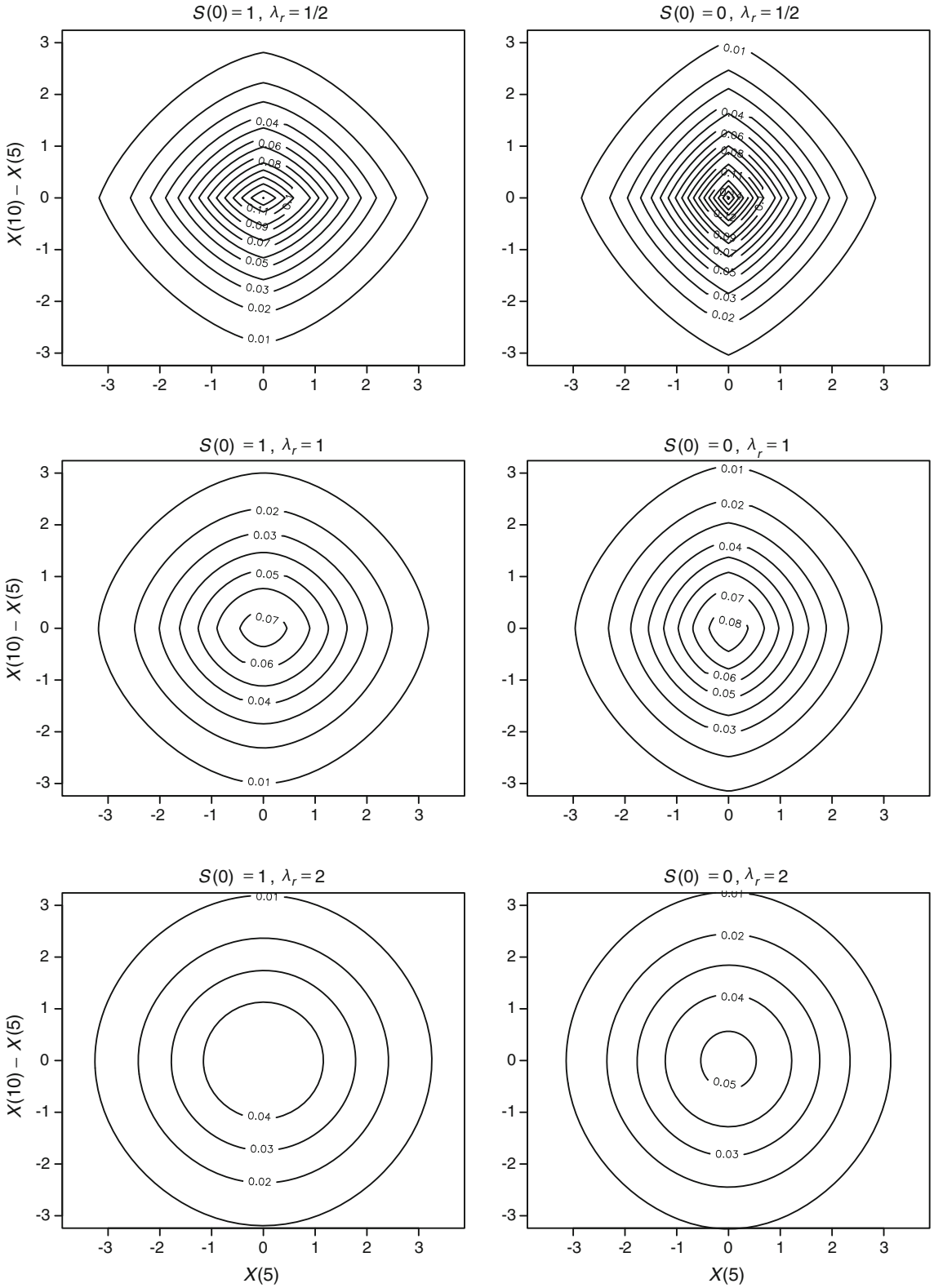

Fig. 4 Contours of the bivariate density of two consecutive increments, $X(5)$ and $X(10) - X(5)$, of a one-dimensional moving–resting process with $\sigma = 1$, $\lambda_m = 1$, and $\lambda_r \in \{1/2, 1, 2\}$. *Left* starting from moving ($S(0) = 1$). *Right* starting from resting ($S(0) = 0$)

Next, assume that $y \neq 0$ and $x \neq 0$, $x \neq y$. Then we do not have any singularities:

$$\Pr(X(u) \in \mathrm{d}x | X(t) = y) = \frac{\Pr(X(u) \in \mathrm{d}x, X(t) \in \mathrm{d}y)}{\Pr(X(t) \in \mathrm{d}y)}, \quad (3)$$

where

$$\frac{\Pr(X(t) \in \mathrm{d}y)}{\mathrm{d}y} = p_m h_m(y,t) + p_r h_r(y,t)$$

and

$$\begin{aligned}&\frac{\Pr(X(u) \in \mathrm{d}x, X(t) \in \mathrm{d}y)}{\mathrm{d}x\mathrm{d}y}\\ &= p_m[h_m(y-x,t-u)h_{mm}(x,u) + h_r(y-x,t-u)h_{mr}(x,u)]\\ &\quad + p_r[h_m(y-x,t-u)h_{rm}(x,u) + h_r(y-x,t-u)h_{rr}(x,u)].\end{aligned}$$

Now, let $y \neq 0$ but $x = 0$. Then at 0 we have an atom with the following weight:

$$\begin{aligned}&\Pr(X(u) = 0 | X(t) = y)\\ &= \frac{\Pr(X(u) = 0, X(t) \in \mathrm{d}y)}{\Pr(X(t) \in \mathrm{d}y)} = \frac{p_r P_r(X(u) = 0, X(t) \in \mathrm{d}y)}{\Pr(X(t) \in \mathrm{d}y)}\\ &= \frac{p_r e^{-\lambda_r u} h_r(y, t-u)}{p_m h_m(y,t) + p_r h_r(y,t)}.\end{aligned}$$

By symmetry in the direction of the process, for $x = y$ and $y \neq 0$, we have

$$\Pr(X(u) = y | X(t) = y) = \frac{p_r e^{-\lambda_r (t-u)} h_r(y,u)}{p_m h_m(y,t) + p_r h_r(y,t)},$$

assuming that p_m and p_r are at the stationary values. This symmetry is obvious, noticing that

$$p_m h_{mr}(y,u) = p_r h_{rm}(y,u),$$

which leads to

$$p_r h_{rr}(y,u) + p_m h_{mr}(y,u) = p_r h_{rm}(y,u) + p_r h_{rr}(y,u).$$

Figure 5 shows the conditional densities of a one-dimensional moving–resting bridge $X(u)$ with $\sigma = 1$, $\lambda_m = 1$, and $\lambda_r \in \{1/2, 1, 2, \infty\}$, at time $u \in \{2, 5, 8\}$ given $X(10) = 9$. The case of $\lambda_r = \infty$ corresponds to a Brownian bridge. Similar to a Brownian bridge, the center of the conditional density of the moving–resting bridge moves towards the ending point $X(10) = 9$ as u increases from 2 to 8. Nevertheless, the conditional density of moving–resting bridges with $\lambda_r < \infty$ has nonzero probability masses at the starting point and the ending point. For smaller λ_r values such as 1/2 and 1, it is obvious that the densities for $u \in \{2, 8\}$ are not differentiable at 0 and 9, the starting and ending points, respectively. The mass probabilities decrease as λ_r increases, which increases the area under the non-degenerate density curve. Eventually, when the mass probability is closer to being exhausted with larger λ_r values, the conditional densities will have heavier tails and resemble more and more those from the Brownian bridge.

Sampling from the bridge

Sampling from the bridge $X(u)$ for $0 < u < t$ given $X(0) = 0$ and $X(t) = x$ can be done by exploiting the connection between a moving–resting process and a Brownian motion. We propose the following algorithm:

1. With probability p_m and p_r, respectively, start from moving and resting phase at $t = 0$.
2. Generate the alternating renewal process with exponential distributions with rate λ_m and λ_r.
3. Remove the resting periods and fill the moving periods with a Brownian bridge with volatility σ.
4. Fill each resting period with its initial location.

The only difference between this algorithm and the algorithm of sampling from a moving–resting process is that the generation of Brownian motion is replaced by generation of Brownian bridge.

This algorithm can be used to generate possible paths given two discretely observed locations at two time points.

Application to animal movements

For a given parameter set (σ, λ_m, λ_r) and the locations of the beginning and the ending point in time interval $(0, t]$, the distribution of the occupation time at any location during this interval can be derived from the bridge model. To get the occupation time density at $x \neq 0$, we need to take the integral of $\Pr(X(u) \in \mathrm{d}x | X(t) = y)/\mathrm{d}x$ with respect to u from 0 to t and then divide the result by t,

$$\frac{1}{t}\int_0^t \Pr(X(u) \in \mathrm{d}x | X(t) = y)\mathrm{d}u/\mathrm{d}x.$$

At $x = 0$ (and $x = y$) we have an atom with the following weight

$$\frac{1}{t}\int_0^t \Pr(X(u) = 0 | X(t) = y)\mathrm{d}u.$$

For illustration, consider a two-dimensional bridge model from a moving–resting process with parameters $\sigma = 1.0$, $\lambda_m = 1$, and $\lambda_r \in \{1/10, 10\}$. Suppose that at the beginning $t = 0$ and at time $t = 10$, an animal is known to be at location $(x_1(0), x_2(0)) = (0, 0)$ and $(x_1(t), x_2(t)) = (9, 3)$, respectively. From the formula above, the occupation distribution has a mass of 0.1123 at each of the two end points for $\lambda_r = 1/10$. This mass is 0.0008 for $\lambda_r = 10$;

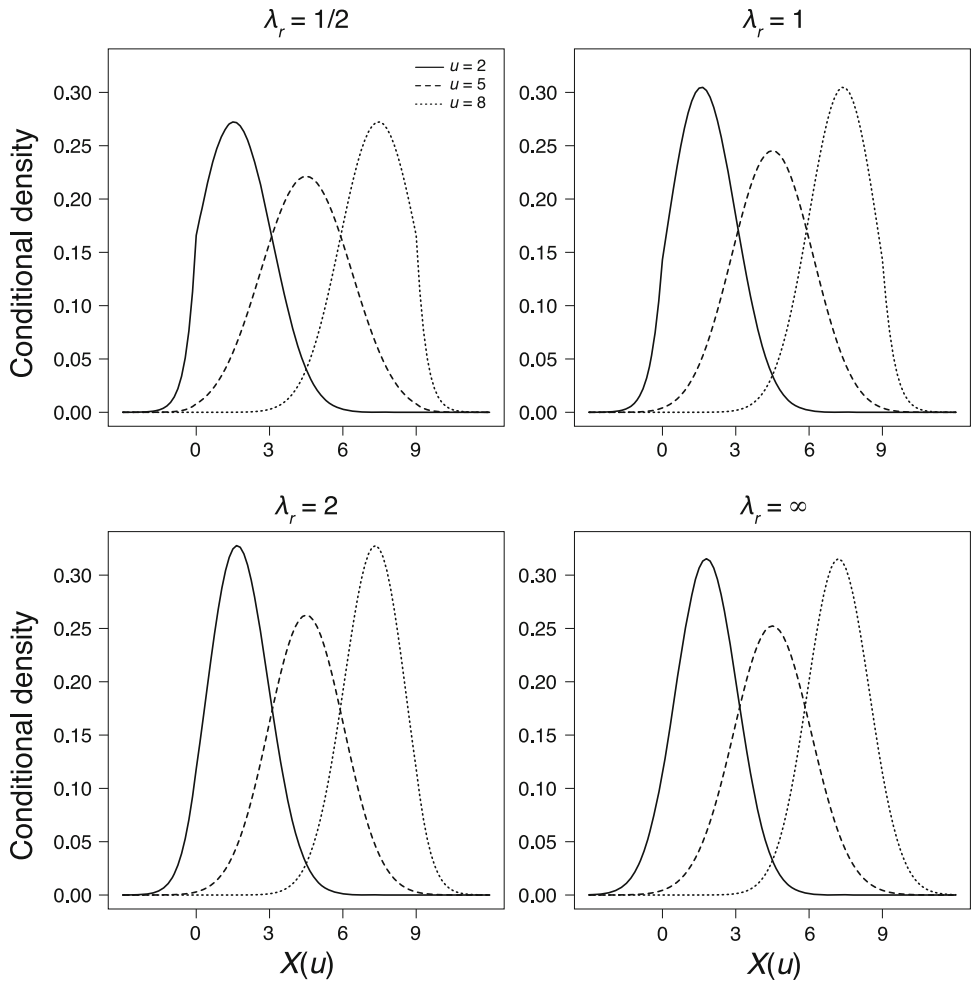

Fig. 5 Conditional densities of a one dimensional moving–resting process with $\sigma = 1$, $\lambda_m = 1$, and $\lambda_r \in \{1/2, 1, 2, \infty\}$, at time $u \in \{2, 5, 8\}$ given $X(10) = 9$

the small mass implies that the occupation distribution is almost the same as that from a BBMM.

The formulas also facilitate calculation of the nonsingular occupation time density for each location (x_1, x_2) on a grid. Combined with the mass at two end points, such calculation can provide contours of the occupation time distribution. Figure 6 shows the contours of the density of the fraction of time spent at each point in a grid region. The three contours in each plot correspond to, respectively, the 50, 80, and 90 % of the occupation time distribution constructed with the highest density approach. Clearly, the density with $\lambda_r = 1/10$ is much tighter than that with $\lambda = 10$, which approximates closely the density from $\lambda = \infty$ as in a BBMM of Horne et al. (2007) without measurement error. The difference is explained by the point mass of 0.1123 at each of the two endpoints when $\lambda_r = 1/10$. Even though the shapes of the contours look similar to those of Horne et al. (2007), there are two important differences. First, our density in the plot does not integrate to one because there are positive masses at (0, 0) and (9, 3). Second, our density is tighter around the line segment that connects the two end points because the animal can spend time resting. The magnitude of the difference is controlled by how much time the animal spent in the resting phase, which is in turn controlled jointly by (λ_m, λ_r). The ratio λ_m / λ_r determines the ratio of the time duration spent in the moving and resting phases on average. The magnitudes of λ_m and λ_r determine how frequently the animal alternates between the two phases.

For comparison, Fig. 6 also shows the contours of the occupation time density for a BBMM with $\sigma = 0.5$. This is of interest because, when fitted to the same data, the estimate of σ from a BBMM will be smaller than that from a moving–resting process. In our real data analysis example, the ratio of the estimates is close to 0.5. The contours are much tighter than those from the moving–resting process with $\lambda_m / \lambda_r = 10$, which is very close to the ratio of the estimates from the real data (10.7). This can be explained by the two directions of the effects of parameter changes: increasing λ_r makes the utilization distribution wider, but decreasing σ makes it tighter. The effect of the first force has a limit; there is little change if λ_r is greater than 10. The

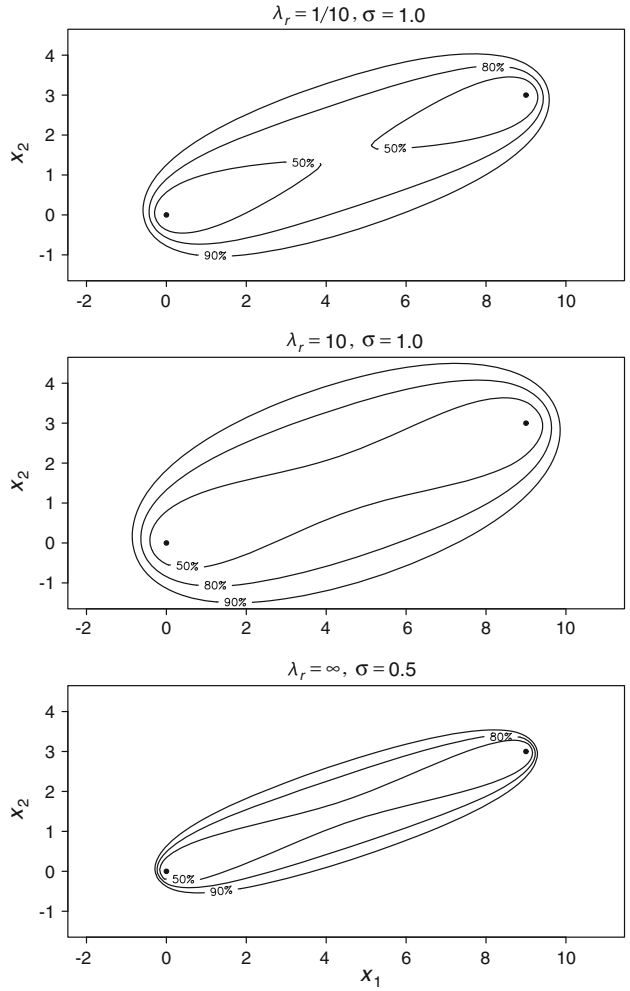

Fig. 6 Contours of the occupation time density in time interval (0, 10), for a two-dimensional bridge model from a moving resting process with parameters $\sigma = 1.0$, $\lambda_m = 1$, and $\lambda_r \in \{1/10, 10\}$ (*top* and *center*), given that $(x_1(0), x_2(0)) = (0, 0)$ and $(x_1(10), x_2(10)) = (9, 3)$. For comparison, the same density from Brownian motion with $\sigma = 0.5$ is also shown (*bottom*). The three contours in each plot correspond to, respectively, the 50, 80, and 90 % of the occupation time distribution constructed with the highest density approach

effect of the second force can make the utilization distribution much tighter as $\sigma \to 0$. The extra parameters λ_m and λ_r do provide more flexible shapes of utilization distributions.

Parameter estimation

Parameter estimation based on discretely observed animal movement data is the first step toward applying the model in practice. It is especially useful for gaining knowledge about cryptic species whose natural history is still unknown. Let $X(t)$, $t = t_0, t_1, \ldots, t_n$, be the observed locations and $S(t)$, $t = t_0, t_1, \ldots, t_n$, be the states of the underlying alternating renewal process for moving and resting. Let $\theta = (\lambda_m, \lambda_r, \sigma)$ be the parameter vector. Depending on whether $S(t)$ is observed or not, parameter estimation can be straightforward or challenging.

$S(t)$ is observed

If the state process $S(t)$ is somehow observed, for example through accelerometers (e.g., Wilson et al. 2006), then the joint process $(X(t), S(t))$ is Markovian, and the full likelihood is available in closed-form. With $X(0) = 0$, the transition density of $(X(t), S(t))$ is

$$f(x(t), s(t)|s(0), \theta) = \begin{cases} h_{mm}(x(t), t) & s(0) = 1,\ s(t) = 1, \\ h_{mr}(x(t), t) & s(0) = 1,\ s(t) = 0, \\ h_{rm}(x(t), t) & s(0) = 0,\ s(t) = 1, \\ h_{rr}(x(t), t) + e^{-\lambda_r t}\delta_0(x) & s(0) = 0,\ s(t) = 0, \end{cases}$$

where the h's are defined in Section "Bridge model from moving–resting process". Note that θ enters all the h's. The likelihood function of the observed data is then

$$L(\theta) = \prod_{i=1}^{n} f(X(t_i) - X(t_{i-1}), S(t_i)|S(t_{i-1}), \theta)$$

This likelihood can be maximized with respect to θ to give the maximum likelihood estimator (MLE) $\hat{\theta}_n$. The usual properties of $\hat{\theta}_n$ such as consistency, asymptotic normality, and asymptotic efficiency hold under regularity conditions. The variance of $\hat{\theta}_n$ can be estimated from the inverse of the Fisher information matrix.

Modern animal tags often include an accelerometer that gives access to information about the activity of animal (Gleiss et al. 2010; Brown et al. 2012; Nathan et al. 2012). If such information does help to determine the moving–resting state $S(t)$ at each observed location, then it can be used in our model and estimation through transition density f. Note that there is no place to use it in the BBMM.

$S(t)$ is not observed

In practice, it is more likely that $S(t)$ is not observed. Then, the observed process $X(t)$ itself is not Markovian and the full likelihood must be constructed from the joint distribution of $X(t)$, $t = t_0, t_1, \ldots, t_n$, which is intractable. One could treat the process $S(t)$, $t = t_0, t_1, \ldots, t_n$, as missing values, and estimate the parameters in a computationally intensive Bayesian approach using general sampling-based inference with Markov chain Monte Carlo (e.g., Robert and Casella 2004). A simpler alternative that does not require full likelihood is the composite likelihood approach (Lindsay 1988).

The composite likelihood approach constructs an objective function by putting pieces of tractable likelihood information together. The objective function, known as composite likelihood, is maximized to give maximum composite likelihood estimator (MCLE) as if it were a likelihood. Under mild conditions, correct specification of the pieces in the composite likelihood leads to consistency and asymptotic normality of the MCLE. It has wide applications where the full joint distribution is unavailable or intractable but lower-order marginal or conditional distributions are known (e.g., Varin 2008; Varin et al. 2011). In our setting, the marginal distribution of one increment, the bivariate joint distribution of two consecutive increments, and the conditional distribution of the bridge given the two end points can all be used to construct different versions of composite likelihood. For illustration, let $\pi(x, t \mid \theta)$ be the marginal density/mass function of one increment at time t for a process starting at $X(0) = 0$, as derived in Section "Bridge model from moving–resting process". A composite likelihood based on π can be constructed as

$$CL(\theta) = \prod_{i=1}^{n} \pi[X(t_i) - X(t_{i-1}),\ t_i - t_{i-1}|\theta].$$

Estimation based on this composite likelihood is implemented in an R package `smam` (Yan and Pozdnyakov 2013). Similar composite likelihoods can be constructed based on the two-increment distribution and the bridge distribution. Note that the pieces in the product are not independent, which is the difference between a composite likelihood and a true likelihood. The variance of the resulting MCLE needs to be estimated with sandwich variance estimators, which is not a trivial task. The finite sample properties of the MCLE from different composite likelihoods also merit further investigation.

To check the performance of the composite likelihood based on π, we conducted a simulation study. Sample paths were generated from a moving–resting process with $\lambda_m = 1/(8 \cdot 60) = 0.00208$, $\lambda_r = 1/(4 \cdot 60) = 0.00417$, and $\sigma = 25$. With time unit minute, these parameters means mean duration of 8 h in the moving stage and 4 h in the resting stage. The sampling frequency is one observation every 20 min. We generated 500 datasets, each with 1000 observations. The parameters were estimated with the composite likelihood. The averages of the estimates 0.00216, 0.00412, and 25.03, with empirical standard deviation 0.00187, 0.00326, and 0.626, respectively, suggesting that the MCLE recovers the true parameter values.

An example

A mature female mountain lion in the Gros Ventre Mountain Range near Jackson, Wyoming was tracked with a GPS collar from 2009 to 2012. The collar was programmed to collect a fix every 8 h but the sampling times were irregular: the sampling intervals had a standard deviation of 6.45 h, ranging from 0.5 to 120 h. There were a total of 3917 observations. Figure 7 shows the easting and northing offsets (meters, UTM) of the lioness's track from her starting position. The lioness's track is similar to the simulated track in Fig. 1, having numerous "plateaus" where the lioness remained very close to one place for several days at a time. For further illustration, we zoomed into the first quarter of 2010 and plotted the distance moved since the last sampling time for each time in the bottom panel of Fig. 7. Most observation times were separated by 8 h. It is clear that at multiple time points, the distance moved since the last sampling time was very close to zero. Field personnel investigated some of these sites and determined them to be places where the lioness consumed a prey item. The lioness typically remained within 250 m of the consumption site during which she exhibited a sallying movement pattern: she repeatedly moved out from the kill and then back, going in different directions. These sallies covered short distances compared to the offsets when the lioness transitioned between consumption sites, so we consider these plateaus to be modeled by resting periods.

We fitted the moving–resting process model to the data using the composite likelihood approach. The parameter estimates are $\hat{\lambda}_m = 3.514$, $\hat{\lambda}_r = 0.328$, and $\hat{\sigma} = 977.6$ m/h. For comparison, we also fitted a Brownian motion model and the estimated parameter is $\hat{\sigma} = 447.9$ m/h. The results suggest that the cat spent much more time resting than moving, with a ratio of 10.7 resting to moving. This is not completely surprising because adult mountain lions spend a majority of their time resting (Beier et al. 1995; Pierce and Bleich 2003; Laundré 2005). When she moved, she moved much faster than what the Brownian motion model suggested, as seen from the difference in $\hat{\sigma}$.

Figure 8 shows the contours of the occupation time density in a 8-h time interval for the female mountain lion estimated from the moving–resting process (left) and the Brownian motion (right), given the locations of two end points (0, 0) and (1.0, 0.8) in km. Although the utilization distributions from the two models are similar in their 95 % contours, they are very different in contours at other levels. The moving–resting model allows the lioness to stay at the two end points with a quite high probability (0.48) and also cover a similar distance to that from the Brownian motion by doubling the volatility parameter (speed).

Discussion

Compared to the BBMM (Horne et al. 2007), the moving–resting process allows the possibility for animals to stay

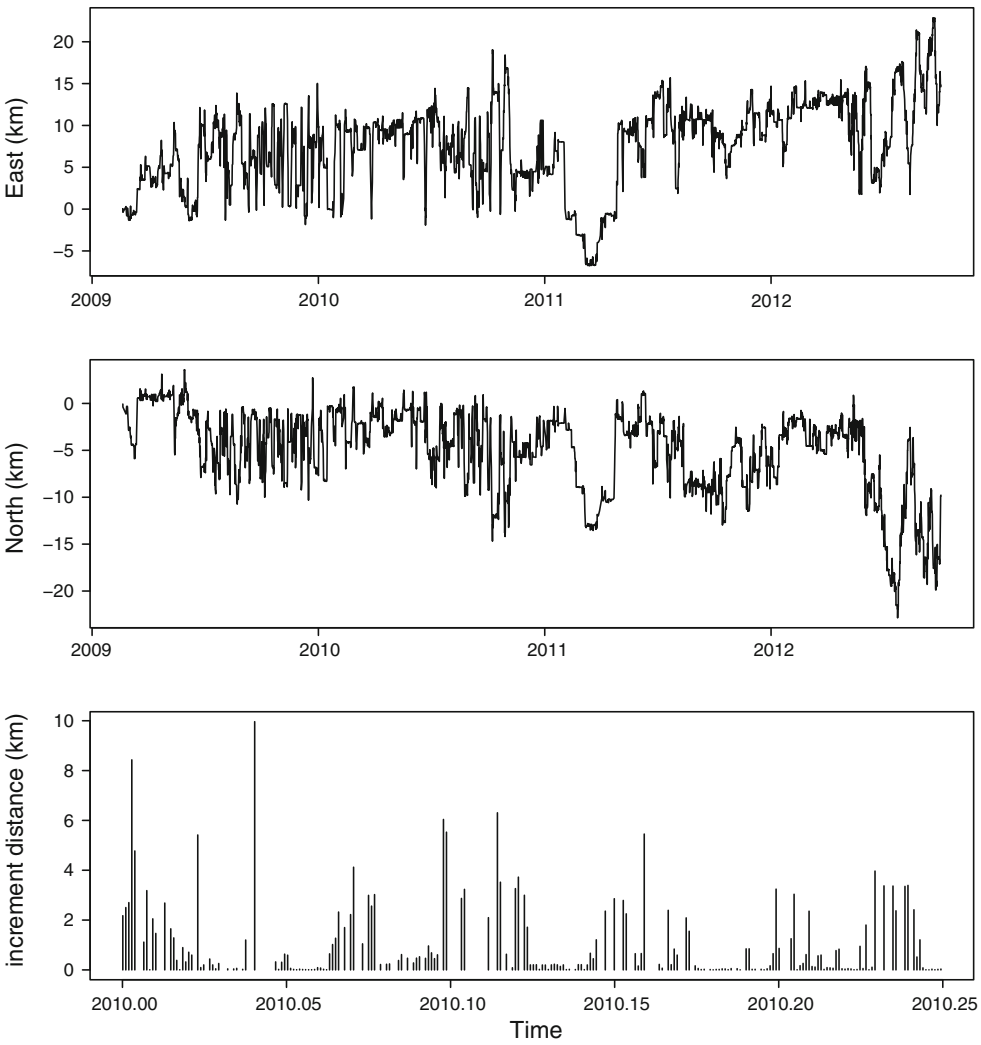

Fig. 7 Locations (*top* and *middle*) of a mature female mountain lion in the Gros Ventre Mountain Range near Jackson, Wyoming tracked with a GPS collar from 2009 to 2012. The *bottom* plot shows the distance moved since the last sampling time for a period zoomed in to the first quarter of 2010

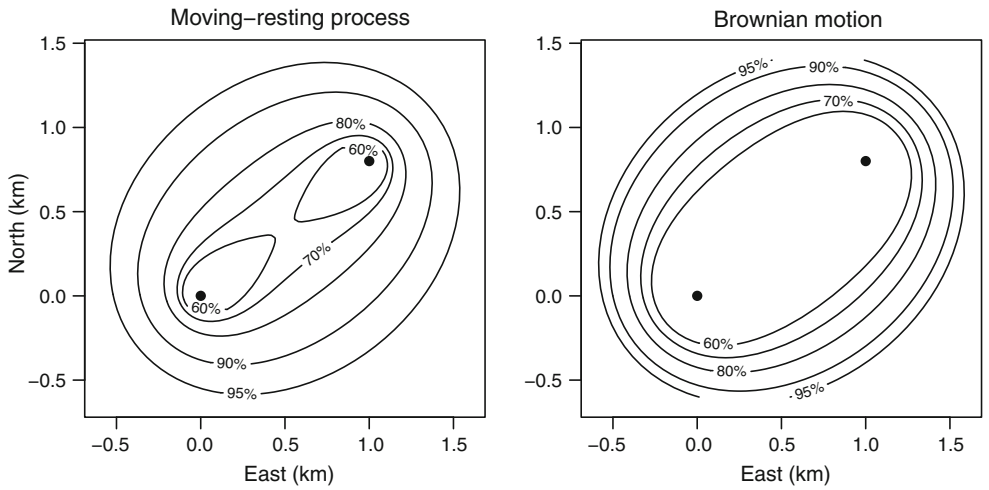

Fig. 8 Contours of the occupation time density in a 8-h time interval for the female mountain lion estimated from the moving–resting process (*left*) and the Brownian motion (*right*), given the locations of two end points (0, 0) and (1.0, 0.8) in km. The probability masses at the two end points sum to 0.48 from the moving–resting model

still, providing a more realistic description of animal behavior. For any given discretely observed animal movement data, three parameters need to be estimated, where the Brownian motion variance measures the mobility of animals in the moving phase, and the two rate parameters of the exponential duration measure the switching between the moving phase and the resting phase. The tractability of the model is facilitated by the exponential distribution assumption of the durations of moving and resting phases, which brings in the memoryless property. The singularity in the distribution does not present any problem with the likelihood approach. Similar to the BBMM, the moving–resting process still assumes that there is a single state of animal behavior: the distributions of time spent moving and resting remain the same over time, and if in moving phase, the movement behavior remains the same. A dynamic extension similar to Kranstauber et al. (2012) can be developed to allow changes in the moving/resting parameters in addition to changes in the Brownian motion variance parameter. This might be helpful when the animal behaviors are cycling.

In home range analysis, our model produces tractable space occupancy probability estimates per pair of position samples. The union of these individual distributions constitutes a rigorous utilization distribution and home range estimate. The utilization distribution determined by our model is spatially explicit but, nonetheless, insensitive to terrain. For kernel-based approaches, one can simply truncate the areas outside of permitted boundaries from the utilization distribution (Christ et al. 2008; Johnson et al. 2008; Benhamou and Cornélis 2010). For movement-based models such as ours or BBMM, it might be reasonable to assume reflective boundaries, in which case, the Brownian motion will be replaced with reflected Brownian motion, and the resulting bridge distribution will be much more complicated depending on the shape of the boundaries. Discrete approximation might be possible (Benhamou 2011). When applied at spatial scales large enough that these exclusions are trivial, we believe the distributions are realistic. Incorporating exclusion areas might be possible with a simulation-based method currently under investigation.

Parameter estimation is simple if $S(t)$ is observed. Resting might be deduced from programming a collar to collect very frequent GPS positions (perhaps one each second for a minute) every so often, or from accelerometers in the collar, but both approaches need extra consideration. The expected user-range error for a timing code based GPS position is on the order of meters (Lawrence-Apfel et al. 2012), so deducing velocity from many fixes very close together in time and space would likely be so dominated by noise to be unhelpful. GPS collars with accelerometers capture brief acceleration snapshots (Markham 2008), which might help to determine the type of no-movement. However, some species [e.g., elk (*Cervus elaphus*)] are adept at keeping the head still while moving and other species frequently raise their head to scan for predators while grazing. Cats might awaken suddenly to groom vigorously for a few moments and then return to sleep. Many behaviors might confound accelerometer data, so their utilization is also unclear. For most practical usage, it is worth further developing estimation methodology that does not use the moving/resting state as input, and studying the properties of the estimator.

An important problem in GPS tracking applications is, what is an optimal sampling interval? GPS wildlife-tracking devices are powered by batteries, which have finite duration capacity dependent upon how frequently the unit is scheduled to acquire a position, and these devices have data stores that eventually become full. Therefore, there is a trade-off between position density (in time) and deployment duration. Modern technology allows the possibility of collecting an essentially continuous set of positions over time, which would give a complete picture of how an animal occupied space—but it may still be too costly for long-term tracking. Deploying tracking collars on wild animals is very expensive. Collars need to be deployed strategically to maximize the information returned on the investment. Researchers usually cannot afford to collect positions with very high frequency; studies last years, not hours. Yet, temporal gaps in recorded positions decrease knowledge of an animal's spatial range. Therefore, rigorous and realistic stochastic utilization distribution models are the best way to achieve a compromise between sampling frequency and study duration to estimate an animal's location between samples. The models presented here incorporate (spatially) stationary periods across a broad range of temporal scales but, interestingly, less so at the finest scales. In general, the method is applicable to macroscopic vertebrates, meaning we believe it is relevant to any vertebrate whose home range is much larger than the expected error in a GPS position (tens of meters), which might exclude certain species such as wood frogs (*Lithobates sylvaticus*) (Rittenhouse and Semlitsch 2009) for example. We note that, although our discussion focused on GPS, it is actually unimportant what positioning technology is used. The method can be applied to fish fitted with radio transmitters and positioned with triangulation. In our model, animal movements in the moving phase are modeled with Brownian motion, which is erratic. Animals do not move erratically at all temporal scales. For example, a deer's path sampled second-to-second might have occasional discontinuous direction changes but, mostly, the path would likely be fairly smooth. The same path sampled hourly can be quite erratic. It is unnecessary—in fact, in some sense it is undesirable—to collect positions so

quickly that they enumerate the trajectory. Determining an optimal sampling frequency—the lowest frequency that delivers a pre-speficied accuracy measure—under the moving–resting process and comparing with that from the BBMM can be an interesting research topic.

Some extensions of the moving–resting process merit further research. Movement data are often subject to observation error, which introduces another source of variation into the modeling framework. Horne et al. (2007) attempted to allow Gaussian noise in their BBMM and derived closed-form expressions for their applications although their method does not provide a satisfactory solution either analytically or computationally (Pozdnyakov et al. 2013). In a more general framework, a state-space model can be developed that combines a model for the observation errors with our model for movement dynamics (e.g., Jonsen et al. 2005; Patterson et al. 2008). Such independent additive error will remove the point mass at zero. Note that, however, it would make the joint process $\{X(t), S(t): t \geq 0\}$ lose its Markov property. The moving–resting process is very easy to simulate, which facilitates agent-based models that take into account both internal state and external factors (e.g., Tang and Bennett 2010). The memoryless property of the process may be unlikely to hold in practice, and extending the Brownian motion part to allow past movement to influence current movement in some memory-based model would be desirable (Smouse et al. 2010).

Acknowledgments This research was partially supported by a Multidisciplinary Environmental Research Award to JY and TM from the Center for Environmental Sciences and Engineering, University of Connecticut. The award supported the graduate assistantship for YC in Spring, 2011. VP and JY thank Dr. Zhiyi Chi for stimulating discussions. The lion data were supplied courtesy of Dr. Mark Elbroch.

References

Beier P, Choate D, Barrett RH (1995) Movement patterns of mountain lions during different behaviors. J Mammal 76:1056–1070

Benhamou S (2011) Dynamic approach to space and habitat use based on biased random bridges. PLoS ONE 6:e14592

Benhamou S, Cornélis D (2010) Incorporating movement behavior and barriers to improve kernel home range space use estimates. J Wildl Manag 74:1353–1360

Brown DD, LaPoint S, Kays R, Heidrich W, Kümmeth F, Wikelski M (2012) Accelerometer-informed GPS telemetry: Reducing the trade-off between resolution and longevity. Wildl Soc Bull 36:139–146

Cane VR (1959) Behavior sequences as semi-Markov chains. J R Stat Soc B 21:36–58

Christ A, Hoef JV, Zimmerman DL (2008) An animal movement model incorporating home range and habitat selection. Environ Ecol Stat 15:27–38

Di Crescenzo A, Di Nardo E, Ricciardi LM (2005) Simulation of first-passage times for alternating Brownian motions. Methodol Comput Appl Probab 7:161–181

Dunn JE, Gipson PS (1977) Analysis of radio telemetry data in studies of home range. Biometrics 33:85–101

Giné GAF, Duarte JMB, Motta TCS, Faria D (2012) Activity, movement and secretive behavior of a threatened arboreal folivore, the thin-spined porcupine, in the Atlantic forest of southern Bahia, Brazil. J Zool 286:131–139

Gleiss AC, Dale JJ, Holland KN, Wilson RP (2010) Accelerating estimates of activity-specific metabolic rate in fishes: Testing the applicability of acceleration data-loggers. J Exp Mar Biol Ecol 385:85–91

Gurarie E, Andrews RD, Laidre KL (2009) A novel method for identifying behavioural changes in animal movement data. Ecol Lett 12:395–408

Heezen KL, Tester JR (1967) Evaluation of radio-tracking by triangulation with special reference to deer movements. J Wildl Manag 31:124–141

Horne JS, Garton EO, Krone SM, Lewis JS (2007) Analyzing animal movements using Brownian bridges. Ecology 88:2354–2363

Hutton TA, Hatfield RE, Watt CC (1976) A method for orienting a mobile radiotracking unit. J Wildl Manag 40:192–193

Johnson DS, Thomas DL, Ver Hoef JM, Christ A (2008) A general framework for the analysis of animal resource selection from telemetry data. Biometrics 64:968–976

Jonsen ID, Flemming JM, Myers RA (2005) Robust state-space modeling of animal movement data. Ecology 86:2874–2880

Kavanau JL (1998) Vertebrates that never sleep: Implications for sleep's basic function. Brain Res Bull 46:269–279

Kranstauber B, Kays R, LaPoint SD, Wikelski M, Safi K (2012) A dynamic brownian bridge movement model to estimate utilization distributions for heterogeneous animal movement. J Anim Ecol 81:738–746

Laundré JW (2005) Puma energetics: a recalculation. J Wildl Manag 69:723–732

Lawrence-Apfel K, Meyer TH, Arifuzzaman K, Ortega IM (2012) An accuracy assessment of global navigation satellite system wildlife-tracking collars in the southern Chilean Patagonia. Anales Instituto Patagonia (Chile) 40:77–85

Lindsay BG (1988) Composite likelihood methods. Contemp Math 80:221–239

Markham A (2008) On a wildlife tracking and telemetry system: a wireless network approach. Ph.d. dissertation, University of Cape Town, South Africa

Marshall AD, Whittington RW (1969) A telemetric study of deer home ranges and behavior of deer during managed hunts. In: Annual Conference of the Southeastern Association Game and Fish Commission, vol 22, pp 30–46

Nathan R, Spiegel O, Fortmann-Roe S, Harel R, Wikelski M, Getz WM (2012) Using tri-axial acceleration data to identify behavioral modes of free-ranging animals: general concepts and tools illustrated for griffon vultures. J Exp Biol 215:986–996

Page ES (1960) Theoretical considerations of routine maintenance. Comput J 2:199–204

Patterson T, Thomas L, Wilcox C, Ovaskainen O, Matthiopoulos J (2008) State-space models of individual animal movement. Trends Ecol Evol 23:87–94

Perry D, Stadje W, Zacks S (1999) First-exit times for increasing compound processes. Commun Stat Stoch Models 15:977–992

Pierce BM, Bleich VC (2003) Mountain lion. In: Feldhamer GA, Thompson BC, Chapman JA (eds) Wild mammals of North America, biology, management and conservation, 2nd edn. Johns Hopkins University Press, Baltimore, pp 744–757

Pozdnyakov V, Meyer TH, Wang YB, Yan J (2013) On modeling animal movements using Brownian motion with measurement error. Ecology. doi:10.1890/13-0532.1

Rittenhouse TAG, Semlitsch RD (2009) Behavioral response of migrating wood frogs to experimental timber harvest surrounding wetlands. Can J Zool 87:618–625

Robert CP, Casella G (2004) Monte Carlo statistical methods, 2nd edn. Springer, New York

Sawyer H, Kauffman MJ, Nielson RM, Horne JS (2009) Identifying and prioritizing ungulate migration routes for landscape-level conservation. Ecol Appl 19:2016–2025

Siegel JM (2009) Sleep viewed as a state of adaptive inactivity. Nat Rev Neurosci 10:747–753

Smouse PE, Focardi S, Moorcroft PR, Kie JG, Forester JD, Morales JM (2010) Stochastic modeling of animal movement. Philos Trans R Soc B Biol Sci 365:2201–2211

Stadje W, Zacks S (2004) Telegraph processes with random velocities. J Appl Probab 41:665–678

Tang W, Bennett DA (2010) Agent-based modeling of animal movement: a review. Geogr Compass 4:682–700

Varin C (2008) On composite marginal likelihoods. Adv Stat Anal 92:1–28

Varin C, Reid N, Firth D (2011) An overview of composite likelihood methods. Stat Sinica 21:5–42

White PJ, Proffitt KM, Mech LD, Evans SB, Cunningham JA, Hamlin KL (2010) Migration of northern Yellowstone elk: Implications of spatial structuring. J Mammal 91:827–837

Wilson RP, White CR, Quintana F, Halsey LG, Liebsch N, Martin GR, Butler PJ (2006) Moving towards acceleration for estimates of activity-specific metabolic rate in free-living animals: the case of the cormorant. J Anim Ecol 75:1081–1090

Wilson RR, Krausman PR, Morgart JR (2009) Behavior and activity budgets of Sonoran pronghorns (*Antilocapra americana sonoriensis)*. Southwest Nat 54:45–54

Yan J, Pozdnyakov V (2013) smam: Statistical Modeling of Animal Movements. URL http://CRAN.R-project.org/package=smam. R package version 0.2-1

Zacks S (2004) Generalized integrated telegraph processes and the distribution of related stopping times. J Appl Probab 41:497–507

Zschille J, Stier N, Roth M (2010) Gender differences in activity patterns of American mink *Neovison vison* in Germany. Eur J Wildl Res 56:187–194